JOC The Journal of Organic Chemistry

Article

pubs.acs.org/joc

Tunable Metal-Catalyzed Heterocyclization Reactions of Allenic Amino Alcohols: An Experimental and Theoretical Study

Benito Alcaide,*[,†] Pedro Almendros,*[,‡] Cristina Aragoncillo,[†] Gonzalo Gómez-Campillos,[†] M. Teresa Quirós,[†] and Elena Soriano[‡]

[†]Grupo de Lactamas y Heterociclos Bioactivos, Departamento de Química Orgánica I, Unidad Asociada al CSIC, Facultad de Química, Universidad Complutense de Madrid, 28040 Madrid, Spain

[‡]Instituto de Química Orgánica General, IQOG-CSIC, Juan de la Cierva 3, 28006 Madrid, Spain

Supporting Information

ABSTRACT: Controlled preparation of 2,5-dihydro-1*H*-pyrroles, 3,6-dihydro-2*H*-pyrans, and pyrroles has been achieved through switchable chemo- and regioselectivity in the metal-catalyzed heterocyclization reactions of allenic amino alcohols. The gold-catalyzed cycloisomerization reaction of *α*-amino-*β*-hydroxyallenes was effective as 5-*endo* cyclization by addition of amino functionality to the distal allene carbon to yield enantiopure 2,5-dihydro-1*H*-pyrroles, whereas their palladium-catalyzed cyclizative coupling reactions furnished 3,6-dihydro-2*H*-pyrans through a chemo- and regioselective 6-*endo* cycloetherification. Conversely, the gold-catalyzed heterocyclization reaction of *β*-amino-*γ*-hydroxyallenes generated exclusively pyrrole derivatives. These results could be explained through a chemo- and regioselective 5-*exo* aminocyclization to the central allene carbon followed by aromatization. Chemo- and regioselectivity depend on both linker elongation as well as the type of catalyst. This behavior can be justified by means of density functional theory calculations.

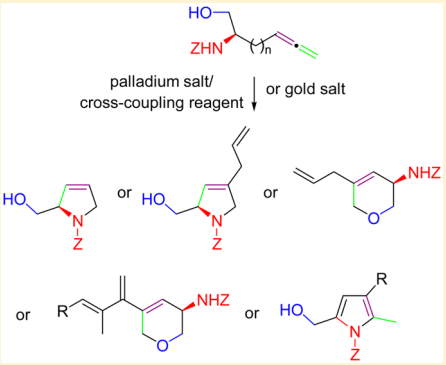

INTRODUCTION

Cycloisomerization reactions have been developed as the most efficient, atom-economical synthetic strategy to build up heterocycles. In particular, catalytic intramolecular addition of a pendant Y−H group to an allene moiety avoids byproduct formation of classical substitution reactions.[1] How to control chemoselectivity to obtain desired adducts over unwanted isomers is the principal issue in these cyclization reactions.

Despite that this performance has previously been reported for allenols and allenamines, related transformations for hydroxy allenamines are undeveloped, probably because of additional chemoselectivity problems. An interesting case of selectivity arises in allenic amino alcohols because two potentially reactive moieties, namely, alcohol and amine, are present in the same substrate. In 2009, the Krause group reported the gold-catalyzed[2] 5-*endo* cycloisomerization of *N*-(buta-2,3-dienyl)hydroxylamines to give *N*-hydroxypyrrolines.[3] Apart from the aminocyclization reaction mentioned above, there exists too few reports on the heterocyclization reactions of allenic amino alcohols. Even so, the switchable[4] synthesis of different heterocycles from the same starting allenic amino alcohol is very attractive but very difficult because each moiety could react to afford diversely sized oxa- or azacycles. Morever, it may also benefit understanding of the reaction mechanisms.[5] We envisioned that a metal-catalyzed heterocyclization reaction of *α*-amino-*β*-hydroxyallenes would produce different 3-, 4-, 5- or 6-membered heterocycles. Depending on both the chemoselectivity (aminocyclization versus oxycyclization) as well as the regioselectivity (*endo-trig* versus *endo-dig* versus *exo-dig* versus *exo-trig* attack), any of the eight possible cycloisomerization adducts could be the reaction products (Scheme 1). In consideration of the importance of both aminocyclization and cycloetherification reactions, we decided to examine the influence of different metal activators on the heterocyclization reaction.

RESULTS AND DISCUSSION

To explore the effects of various complexes on the metal-catalyzed heterocyclization reaction of allenic amino alcohols, *α*-amino-*β*-hydroxyallene **1a** and *β*-amino-*γ*-hydroxyallenes **2a**,**b** were synthesized in optically pure form. Starting allene **3** was made from the corresponding alkyne by treatment with paraformaldehyde in the presence of diisopropylamine and copper(I) bromide (Crabbé reaction) using our previously described methodology.[6] Starting allenes **4a**,**b** were obtained from Garner's aldehyde via coupling with propargyl bromides promoted by indium, followed by protection of the hydroxyl functionality in the form of methyl ether.[7] Precursors for the heterocycle formation, enantiopure allenic amino alcohols **1a** and **2a**,**b** were smoothly obtained in excellent yields by $BiCl_3$-catalyzed aminal cleavage (Scheme 2). Unfortunately, we faced significant difficulties at the purification stage in the case of highly polar substrates **2a**,**b**. Chromatography, even with

Received: April 25, 2016
Published: July 27, 2016

DOI: 10.1021/acs.joc.6b00934
J. Org. Chem. 2016, 81, 7362−7372

Scheme 1. Possible Cycloisomerizations that Can Occur in α-Amino-β-hydroxyallenes

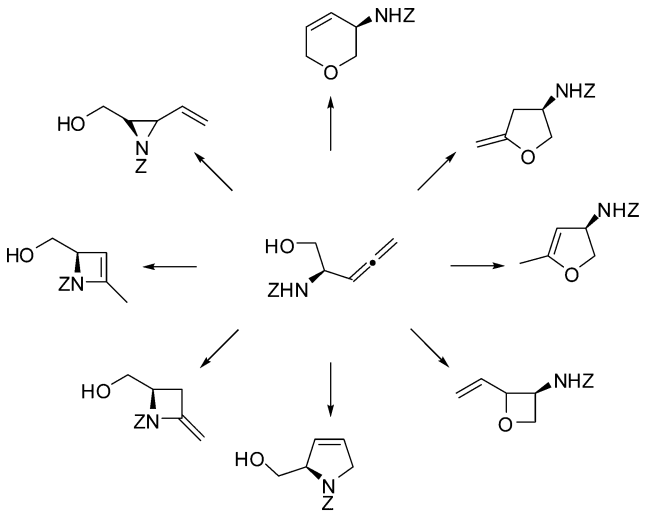

neutralized silica gel or alumina, resulted in decomposition products. Consequently, we devised a one-pot sequence from oxazolidine-derived allenes **4a**,**b**, avoiding the purification of β-amino-γ-hydroxyallenes **2a**,**b**. Thus, it was our hope that the resulting crude products displayed sufficient purity to be engaged in the metal-catalyzed cyclization step.

Next, we targeted the use of metal catalysis to the selective preparation of heterocycles starting from allenic amino alcohols. Initially, it was hoped that a catalytic activation strategy could be developed through the use of noble metal salts. In the investigation of the reaction conditions, α-amino-β-hydroxyallene **1a** was chosen as the model substrate. First, the effect of the catalyst on the model reaction was examined. Fortunately, a variety of gold and platinum catalysts were applied with success to α-amino-β-hydroxyallene **1a**. These reactions were completely selective for the formation of 2,5-dihydro-1*H*-pyrrole **5a** (Table 1). When the reaction was catalyzed by $[PtCl_2(CH_2{=}CH_2)]_2$ or $PtCl_2$/AgOTf, comparable results of azacycle **5a** were obtained (Table 1). However, the addition of Gagosz' catalyst $[(Ph_3P)AuNTf_2]$ provided lower yield of the cycloisomerization product (Table 1). To our delight, the use of a gold(III)-based catalyst, such as $AuCl_3$, enhanced the hydroamination reaction. Thus, 2,5-dihydro-1*H*-pyrrole **5a** could be isolated after purification by column chromatography in 77% yield after $AuCl_3$ treatment. A screening of solvents (toluene, polyethylene glycol 400, 1,2-dichloroethane) revealed that the reaction is best performed in dichloromethane. The above outcome could be rationalized invoking a 5-*endo* cycloisomerization by chemo- and regiospecific addition of the amino group to the terminal allene carbon.[8]

A need of modern organic synthesis is to investigate how different types of molecules can be created from the same starting material merely through catalyst choice. Thus, having found a solution for the selective allenic aminocyclization, our next aim was to study the catalyst-controlled chemoselective heterocyclization of allenic amino alcohols to obtain oxacycles. Our initial investigations on Pd-catalyzed chemodifferentiation reactions focused on the heterocyclization of α-amino-β-hydroxyallene **1a** with allyl bromide.[9] Worthy of note, the reaction took place with $PdCl_2$ catalysis, affording 3,6-dihydro-2*H*-pyran-3-amine derivative **6a** in fair yield (Scheme 3). Disappointingly, along with cyclic ether **6a**, dihydropyrrole **7a** was also obained as a minor product. Fortunately, isomeric heterocycles **6a** and **7a** were easily separable by flash chromatography. The formation of dihydropyran **6a** can be somehow explained through a chemoselective 6-*endo*-*trig* allenic oxycyclization followed by cross-coupling.

We thought it would be of interest to apply α-amino-β-hydroxyallene **1a** to our previously developed palladium-catalyzed heterocyclization/cross-coupling sequence between α-allenols and α-allenic esters.[10] Gratifyingly, it was observed that these reaction conditions using α-allenic esters **8** were compatible with substrate **1a**, resulting in the formation of the desired oxacycles **9** in fair yields with complete regio- and chemoselectivity (Scheme 4). The ^1H NMR spectra of the crude reaction mixtures show the presence of oligomeric material but did not reveal the formation of any cyclization/cross-coupling adducts different than products **9**.

Lanthanide amido complexes have shown remarkable success in catalyzing both hydroamination[11] and hydroalkoxylation reactions.[12] The above precedents suggest that lanthanide-based catalysts may be effective for the cycloisomerization reaction of allenic amino alcohols. In marked contrast, it was found that the *N*-Boc cleavage of α-amino-β-hydroxyallene **1a** occurred using lanthanum bis(trimethylsilyl)amide as promoter (Scheme 5). Of note, the allene moiety in product **1b** remained intact despite its inherent reactivity. To the best of our knowledge, such controlled reactivity has not been reported previously.

Scheme 2. Preparation of Enantiopure Allenic Amino Alcohols 1 and 2

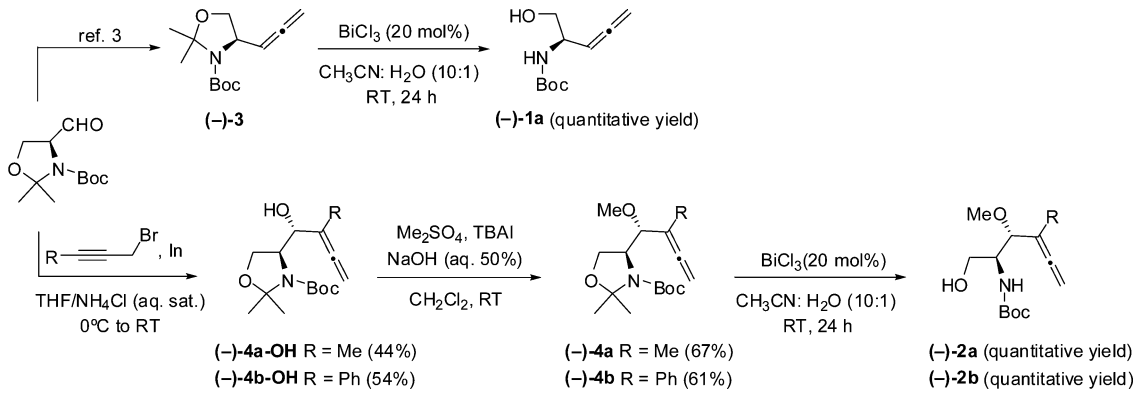

DOI: 10.1021/acs.joc.6b00934
J. Org. Chem. 2016, 81, 7362–7372

Table 1. Selective Aminocyclization Reaction of α-Amino-β-hydroxyallene 1a under Modified Metal-Catalyzed Conditions

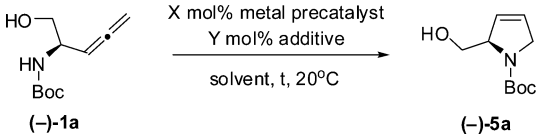

(–)-1a (–)-5a

entry	metallic salt (X mol %)	additive (Y mol %)	solvent/t (h)	yield[d]
1	$PtCl_2$ (5)	AgOTf (5)	CH_2Cl_2 /23	59
2	$[PtCl_2(CH_2=CH_2)]_2$ (5)	TDMPP[a] (10)	CH_2Cl_2/23	52
3	$[(Ph_3P)AuNTf_2]$ (5)		DCE[b]/3	20
4	$AuCl_3$ (5)		toluene/5	68
5	$AuCl_3$ (5)		PEG-400[c]/4	49
6	$AuCl_3$ (5)		DCE/3	75
7	$AuCl_3$ (5)		CH_2Cl_2/3	77

[a]TDMPP = tris(2,6-dimethoxyphenyl)phosphine. [b]DCE = 1,2-dichloroethane. [c]PEG = polyethylene glycol 400. [d]Yield of pure, isolated product with correct analytical and spectral data.

Scheme 3. Palladium-Catalyzed Preparation of Dihydropyran 6a and Dihydropyrrole 7a

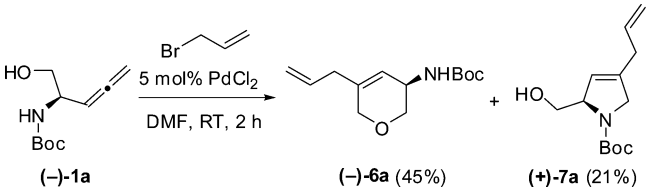

(–)-1a (–)-6a (45%) (+)-7a (21%)

Scheme 4. Palladium-Catalyzed Preparation of Dihydropyrans 9 where PMP = 4-MeOC$_6$H$_4$

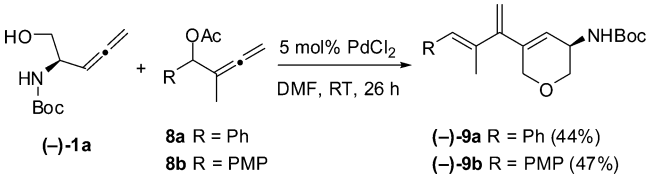

(–)-1a
8a R = Ph
8b R = PMP
(–)-9a R = Ph (44%)
(–)-9b R = PMP (47%)

Scheme 5. Lanthanum-Catalyzed Preparation of α-Amino-β-hydroxyallene 1b

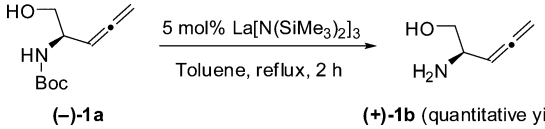

(–)-1a (+)-1b (quantitative yield)

To address the selectivity issue on the metal-catalyzed heterocyclization reaction of allenic amino alcohols, we further investigated additional substrate **1b**. We were pleased to observe that α-amino-β-hydroxyallene **1b** also worked well under the optimized catalytic conditions of Table 1 and Schemes 3 and 4. Thus, gold-catalyzed cycloisomerization and palladium-catalyzed cyclization/coupling reactions lead to the controlled formation of heterocycles **5b**–**7b** and **10a**,**b** in slightly higher yields (Scheme 6). Dendralenic products **10** are potential precursors for more complex structures through the diene-transmissive Diels–Alder reaction.[13]

Next, we focused on finding a heterocyclization procedure for functionalized allenes **2a**,**b** that could be both regio- and chemoselective. β-Amino-γ-hydroxyallenes **2a**,**b** have diverse reactive sites at which two different transformations (*N*- vs *O*-cyclization) can take place. Gold(I)-based complexes were the best catalysts among several complexes screened ($AuCl_3$, $PtCl_2$, $PdCl_2$, $PtCl_2(CH_2=CH_2)]_2$). A number of gold(I) catalysts were tested to reveal that $[(Ph_3P)AuNTf_2]$ was the catalyst of choice. The best result was obtained from a reaction of **2a** using $[(Ph_3P)AuNTf_2]$ (5 mol %) in dichloromethane, producing *tert*-butyl 5-(hydroxymethyl)-2,3-dimethyl-1*H*-pyrrole-1-carboxylate **11a** in 53% isolated yield (Scheme 7). When the present reaction was conducted with allenic amino alcohol **2b**, pyrrole derivative **11b** was also exclusively produced (Scheme 7). Unfortunately, extensive decomposition was observed on sensitive pyrroles **11** during purification by flash chromatography, which may be responsible for the moderate isolated yields. The gold-catalyzed heterocyclization reaction of β-amino-γ-hydroxyallenes **2** shows the same chemoselectivity but different regioselectivity as that observed under gold catalysis

Scheme 6. Chemo- and Regiocontrol in the Metal-Catalyzed Heterocyclization Reactions of α-Amino-β-hydroxyallene 1b

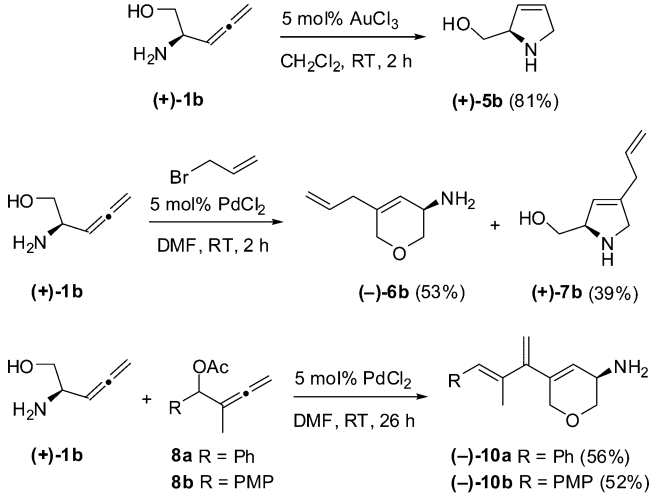

(+)-1b (+)-5b (81%)
(+)-1b (–)-6b (53%) (+)-7b (39%)
(+)-1b
8a R = Ph
8b R = PMP
(–)-10a R = Ph (56%)
(–)-10b R = PMP (52%)

Scheme 7. Gold-Catalyzed Preparation of Pyrroles 11

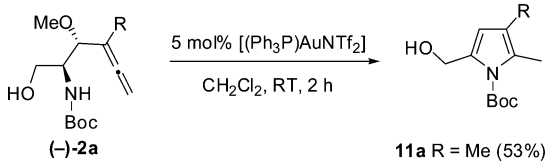

(–)-2a
(–)-2b
11a R = Me (53%)
11b R = Ph (40%)

DOI: 10.1021/acs.joc.6b00934
J. Org. Chem. 2016, 81, 7362–7372

for α-amino-β-hydroxyallenes **1**, that is, the initial cyclization takes place by selective nucleophilic addition of the amino group to the activated central allene carbon. By contrast, the cyclization of β-amino-γ-hydroxyallenes **2a,b** was not as rewarding when they were treated with allyl bromide using a Pd-based catalytic system. Palladium salts, which were effective for the oxycyclization reaction of allenic amino alcohols **1a,b**, gave rise to complex reaction mixtures. These results clearly show that metal-catalyzed aminocyclization is preferred over cycloetherification for β-amino-γ-hydroxyallenes **2**. Pyrrole formation could be explained through a 5-*exo* cyclization by chemo- and regioselective attack of the amino group to the central allene carbon, followed by elimination of methanol with concomitant aromatization.

A possible mechanism for the catalytic achievement of 2,5-dihydro-1*H*-pyrroles **5** involving a gold-based carbophilic π-acid may proceed through initial coordination of the metal to the distal double bond of α-amino-β-hydroxyallenes **1** leading to species **1-Au**. Next, chemo- and regioselective 5-*endo*-trig allenic aminoauration forms zwitterionic dihydropyrroles **12**. Loss of HCl in intermediates **12** generates neutral alkenylmetal species **13**. Protonolysis of the carbon−gold bond of **13** liberates 2,5-dihydro-1*H*-pyrroles **5** with concomitant regeneration of the Au(III) catalytic species (Scheme 8).

Scheme 8. Mechanistic Explanation for the Gold-Catalyzed Cycloisomerization Reaction of α-Amino-β-hydroxyallenes 1

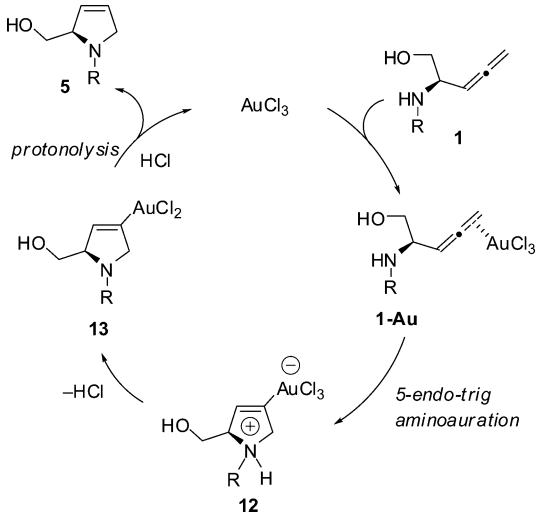

A mechanistic hypothesis for the achievement of 3,6-dihydro-2*H*-pyrans **9** and **10** from α-amino-β-hydroxyallenes **1** is outlined in Scheme 9. Chemo- and regiocontrolled palladium(II)-catalyzed oxypalladacyclization of the amino-β-hydroxyallene molecule **1** produces a palladadihydropyran species **14**, which then suffers a cross-coupling reaction with α-allenic ester **8**. Alkenyl palladium(II) species **14** reacted with the central allene carbon of **8** in a regioselective fashion, giving rise to intermediates **15**. Subsequently, buta-1,3-dienyl 3,6-dihydro-2*H*-pyran-3-amines **9** and **10** are formed as single *E*-isomers through *trans*-β-deacetoxypalladation. The metal catalyst is reformed at the same time. Notably, the heteropalladation of α-amino-β-hydroxyallenes **1** to form corresponding 3,6-dihydropyranyl palladium species **14** is totally chemoselective toward the allenol functionality. We did not observe the formation of

Scheme 9. Mechanistic Explanation for the Palladium-Catalyzed Oxycyclization/Cross-Coupling Sequence between α-Amino-β-hydroxyallenes 1 and α-Allenic Esters

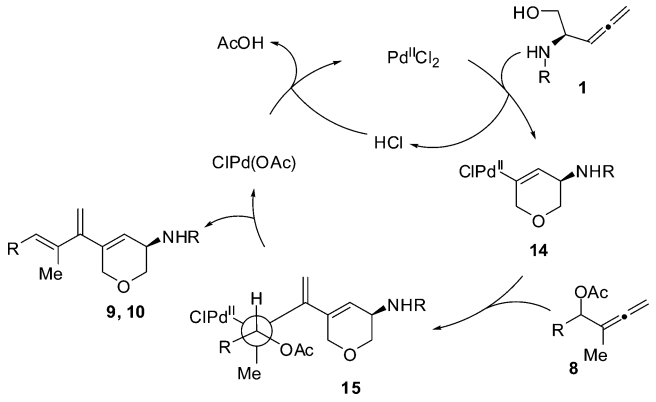

azacycles from the aminocyclization of the allenamine functionality in **1**.

Scheme 10 outlines a mechanistic proposal for the achievement of pyrroles **11** from allenic amino alcohols **2**.

Scheme 10. Mechanistic Explanation for the Gold-Catalyzed Aminocyclization Reaction of β-Amino-γ-hydroxyallenes 2

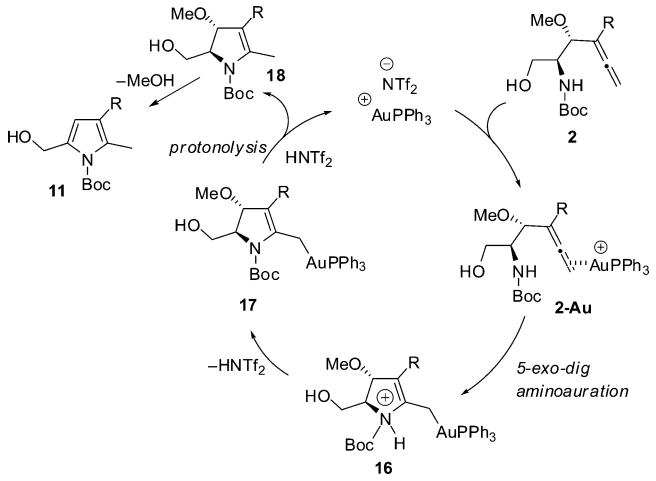

Initial Au^I-coordination to the 1,2-diene moiety gives allenegold complex **2-Au**, which suffers a chemo- and regioselective 5-*exo* aminocyclization reaction to give intermediate auradihydropyrrolium **16**. Loss of proton generates neutral species **17**, which followed by protonolysis of the carbon−gold bond affords dihydropyrroles **18** with concurrent regeneration of the gold catalyst. Heterocycles **18** then suffer a methanol elimination to give the pyrrole products **11**.

To obtain further insights into the chemo- and regioselectivity, as well as the reaction pathway, we performed a density functional theory (DFT) study.

As a model reaction, we have selected precursor **1b**. Table 2 summarizes the activation barriers and relative energies for the possible heterocyclization steps for both the amino and alcohol functionalities from the allene−metal complexes **1b-Au$_D$** and the less stable **1b-Au$_P$**. These complexes are formed by coordination of the distal and proximal alkene bonds of the allene to the catalyst, respectively.

According to the calculated values, the lowest-energy transition structure for the Au(III)-catalyzed heterocyclization

DOI: 10.1021/acs.joc.6b00934
J. Org. Chem. 2016, 81, 7362−7372

Table 2. Relative Free-Energy Values [M06/def2-QZVP/PCM, in kcal mol^{-1}] for the Possible Au-Catalyzed Heterocyclization Steps of 1b

complex		mode	$\Delta G^{\#}$	ΔG
1b-Au$_D$	aminocyclizations	4-*exo-dig*-	3.7	−13.4
		5-*endo-trig*-	2.6	−17.7
	oxycyclizations	5-*exo-dig*-	8.6	−12.2
		6-*endo-trig*-	6.1	−2.3
1b-Au$_P$	aminocyclizations	3-*exo-trig*-	7.8	−15.0
		4-*endo-dig*-	13.3	−9.1
	oxycyclizations	5-*endo-dig*-	10.8	−10.5
		4-*exo-trig*-	12.8	6.8

is found for **TS1$_{5\text{-endo-trig}}$**, which belongs to the 5-*endo-trig* cyclization.[1,14] Moreover, it drives to the most stable Au σ-alkenyl zwitterionic intermediate **I$_{5\text{-endo-trig}}$**. Other plausible transition structures for the intramolecular nucleophilic attack of the alcohol or amine on the triggered allene show higher barriers than that of **TS1$_{5\text{-endo-trig}}$** ($\Delta\Delta G^{\#}$ = 1.1−10.7 kcal mol^{-1}). The formation of the heterocyclization intermediates is exergonic for all; only one exception is found, as the strained attack of the β-allenol group onto the central allene position, 4-*exo-trig* cyclization, is slightly endergonic. In fact, the formation of the most stable Au σ-alkenyl intermediate **I$_{5\text{-endo-trig}}$** is the most exergonic process (−17.7 kcal mol^{-1}), pointing to a moderately irreversible character of this heterocyclization mode.

These results agree with the experimentally observed selective formation of 3-pyrroline **5b** and propose kinetic and thermodynamic control of the chemo- and regioselective intramolecular aminocyclization. However, according to previous estimation of the reaction mechanism by us[15] and others,[16] the rate-determining step would be the 1,3-H migration to form the product, which is assisted by the metal complex and proceeds stepwise: release of HCl and Au−C bond excision by protonolysis with HCl to end the cycle and restore the active catalyst.[17]

For the formation of **5b**, the loss of HCl from **I$_{5\text{-endo-trig}}$** produces the neutral complex **I2$_{5N}$-Au** in an endergonic process (ΔG = +16.2 kcal mol^{-1}). To end, protonolysis of the C−Au bond yields **5b-Au** via the transition state **TS3$_{5N}$-Au** with an activation energy of $\Delta G^{\#}$ = +4.9 kcal mol^{-1}. Thus, according to the calculated higher energy barriers, the 1,3-H migration would be the bottleneck of the Au-catalyzed formation of **5b** (Figure 1).

For the Pd-catalyzed process, the calculations also suggest that the 5-*endo-trig* heterocyclization by nucleophilic attack of the α-amino moiety to the terminal allene carbon of the most stable complex, **1b-Pd$_D$** (by 0.8 kcal mol^{-1}) (via **TS1$_{5\text{-endo-trig}}$**) (Table 3), is the favored ring-closure step both from the kinetic and thermodynamic perspectives in view of the higher activation energy barriers ($\Delta\Delta G^{\#}$ = 4.8−18.1 kcal mol^{-1}) and

Table 3. Relative Free-Energy Values [M06/def2-QZVP/PCM, in kcal mol^{-1}] for the Possible Pd-Catalyzed Heterocyclization Steps of 1b

complex		mode	$\Delta G^{\#}$	ΔG
1b-Pd$_D$	aminocyclizations	4-*exo-dig*-	9.7	−9.2
		5-*endo-trig*-	2.3	−12.9
	oxycyclizations	5-*exo-dig*-	15.8	−8.1
		6-*endo-trig*-	7.1	4.1
1b-Pd$_P$	aminocyclizations	3-*exo-trig*-	11.7	−8.1
		4-*endo-dig*-	19.9	−7.7
	oxycyclizations	5-*endo-dig*-	19.0	−3.0
		4 *exo-trig*-	20.4	12.8

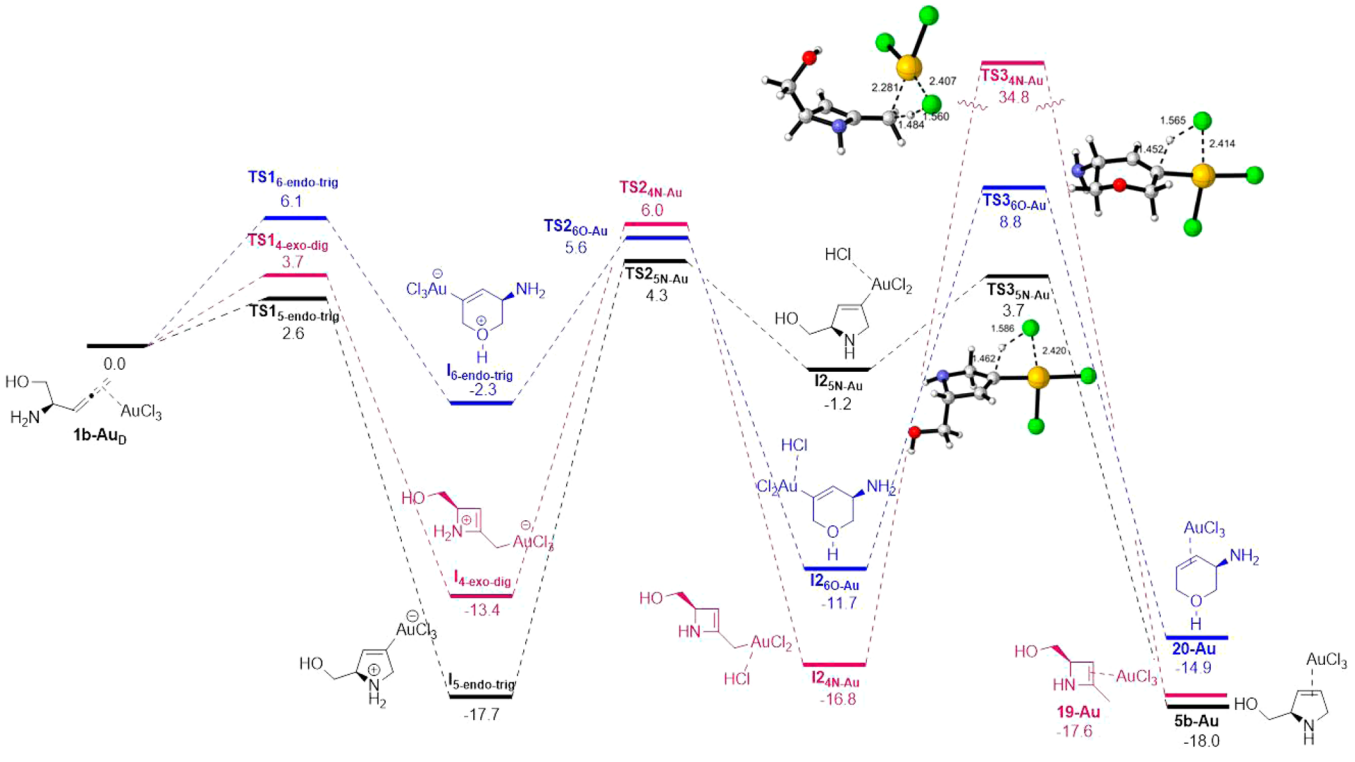

Figure 1. Calculated free-energy profile [M06/def2-QZVP/PCM, in kcal mol^{-1}] for some plausible Au-catalyzed reactions of **1b**.

DOI: 10.1021/acs.joc.6b00934
J. Org. Chem. 2016, 81, 7362−7372

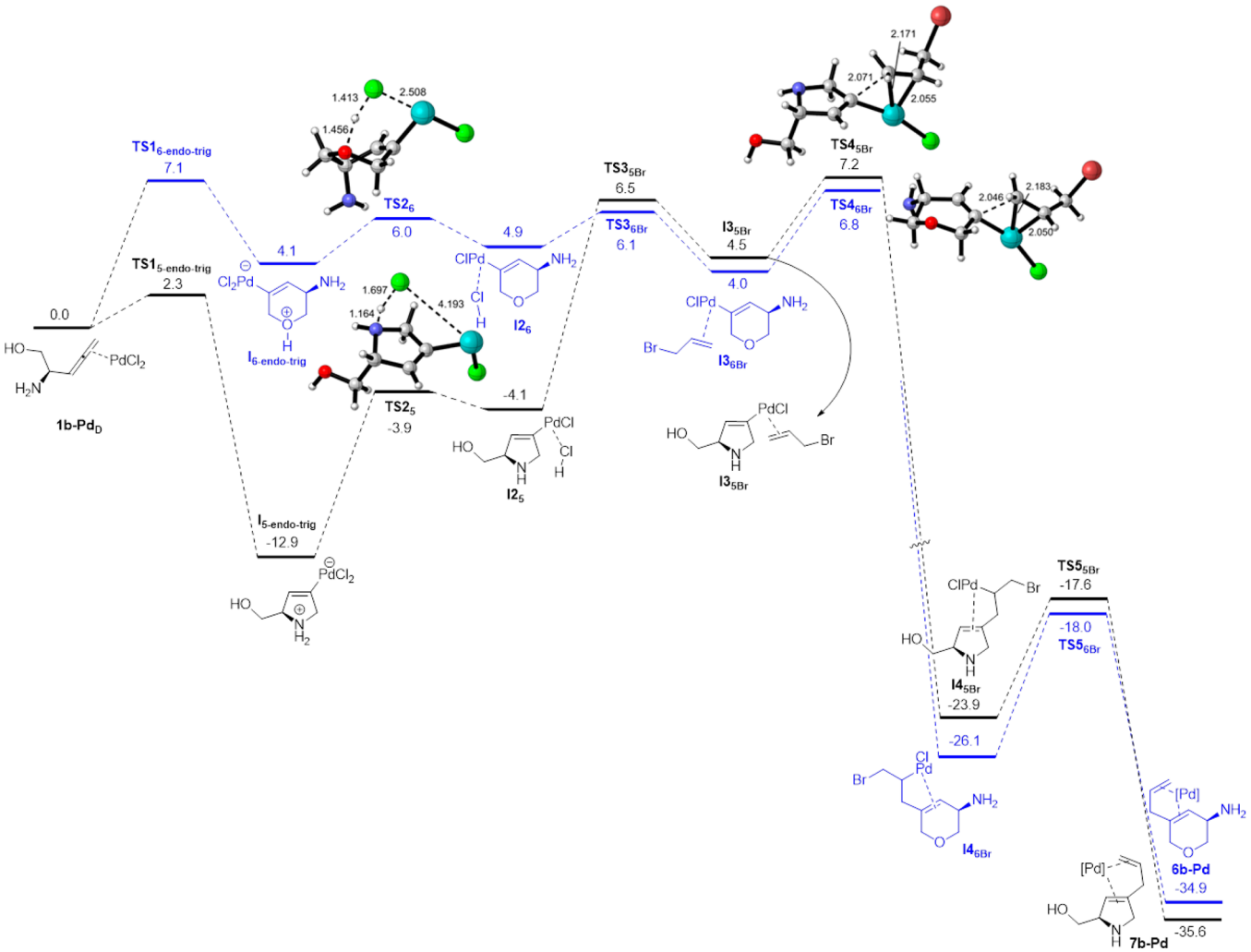

Figure 2. Calculated free-energy profile [M06/def2-QZVP/PCM, in kcal mol^{-1}] for the Pd-catalyzed heterocyclization/cross-coupling reaction of **1b** with allyl bromide to form **6b** (blue) and **7b** (black).

the lower exergonicity ($\Delta\Delta G$ = 3.7−25.7 kcal mol^{-1}) computed for other plausible heterocyclizations. Notably, the *endo-trig* cyclization by nucleophilic attack of the β-alcohol on the terminal allene carbon, through **TS1**$_{\text{6-endo-trig}}$, also shows a low activation barrier, although it is 4.8 kcal/mol higher, which unfortunately contrasts with the experimental observations.

On other hand, the results depicted in Scheme 6 suggest that the selectivity of the Pd-catalyzed process depends on the nature of the coupling alkene. Thus, in the presence of allyl bromide, the kinetically favored formation of the **I**$_{\text{5-endo-trig}}$ and **I**$_{\text{6-endo-trig}}$ alkenyl intermediates would undergo a cross-coupling reaction to form **7b** and **6b**, respectively, whereas in the presence of α-allenic ester, the formation of oxacycles **10** takes place with complete regio- and chemoselectivity. To account for these observations and apparent discrepancies, we have performed a deeper analysis.

The cross-coupling with allyl bromide from alkenyl intermediate **I**$_{\text{6-endo-trig}}$ takes place as follows (Figure 2). After the loss of HCl through **TS2**$_6$ (+6.0 kcal mol^{-1} above **1b-Pd**$_D$), the Pd-coordinated HCl is easily moved by the entering allyl bromide in a probable fast ligand-interchange displacement mechanism to yield the palladium complex **I3**$_{6Br}$. This step is slightly endergonic (ΔG = −0.9 kcal mol^{-1}) and has a low activation barrier (1.2 kcal mol^{-1}). This species evolves into complex **I4**$_{6Br}$ via the nearly planar four-membered transition structure **TS4**$_{6Br}$, a saddle point related to the insertion of the allylic halide C═C bond into the Pd-alkenyl bond to yield σ-C−Pd intermediate **I4**$_{6Br}$ and the formation of a new carbon−carbon bond. This intermediate is formed in a highly exergonic step (−30.1 kcal mol^{-1}) with a low activation barrier (2.8 kcal mol^{-1}). A final elimination step yields the complexed dihydropyran **6b-Pd** in an exergonic step (by −8.8 kcal mol^{-1}) through **TS5**$_{6Br}$ (−18.0 kcal mol^{-1}). Overall, the reaction is highly exergonic, and the cyclization and coupling steps constitute the bottleneck of the transformation.

Earlier computational results on palladium-catalyzed reactions have revealed that, in the presence of an unsaturated reactant, the cross-coupling from the alkenyl intermediate is favored over a proton shift process to yield protonolysis products.[12d,18] Expectedly, the competitive protonolysis step from **I2**$_6$ involves a less favored process both from kinetic and thermodynamic viewpoints because our calculations reveal a higher activation barrier (transition structure 11.9 kcal mol^{-1} above **1b-Pd**$_D$) and less exergonicity (−14.4 kcal/mol) than the coupling process, in agreement with the experimental absence of the protonolysis product.

The formation of 3-pyrroline **7b** follows the equivalent pathway after azacyclization (Figure 2), namely, loss of HCl,

DOI: 10.1021/acs.joc.6b00934
J. Org. Chem. 2016, 81, 7362−7372

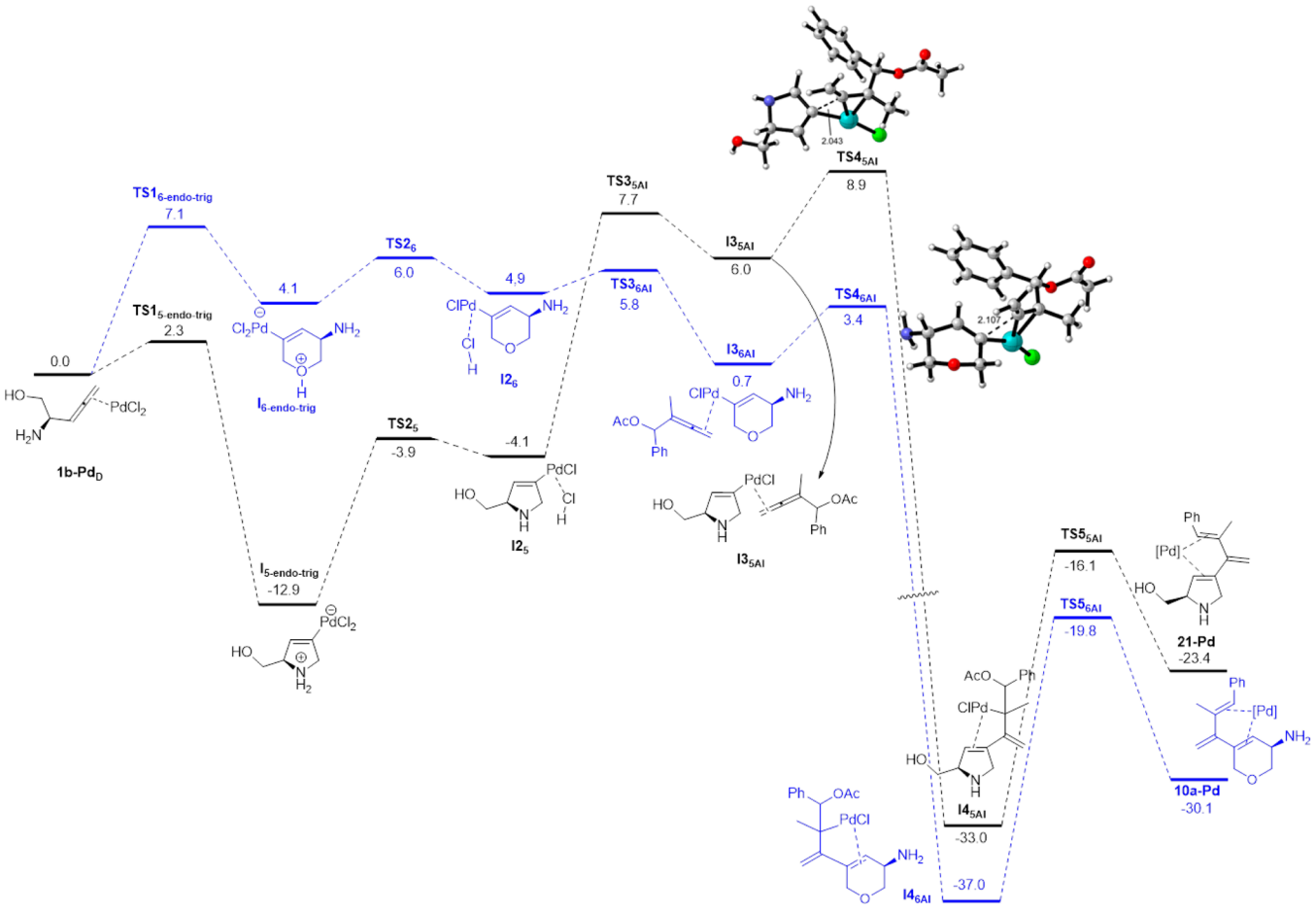

Figure 3. Comparison of the free-energy profiles [M06/def2-QZVP/PCM, in kcal mol^{-1}] for the Pd-catalyzed heterocyclization/cross-coupling reaction of **1b** with α-allenic acetate **8a** to yield **10a** (blue) and the undetected dihydropyrrole product **21** (black).

ligand displacement from the metal coordination sphere, insertion of the C=C bond of the allylic halide into Pd–alkyl bond to yield a σ-C–Pd intermediate, and finally a β-elimination step. First, the lower activation barrier for the HCl release is likely due to the lower steric distortion needed to attain the transition state, whereas the higher stability of $\mathbf{I2_5}$ is due to the strong H-bond of the formed HCl with the amine group. This complex can coordinate the allyl bromide to produce the allyl-palladium complex $\mathbf{I3_{5Br}}$, which is 0.5 kcal mol^{-1} less stable than $\mathbf{I3_{6Br}}$, through transition structure $\mathbf{TS3_{5Br}}$ showing an energy 0.4 kcal mol^{-1} higher than that of the dihydropyran counterpart ($\mathbf{TS3_{6Br}}$). This intermediate species evolves into complex $\mathbf{I4_{5Br}}$ by formation of the new carbon–carbon bond via the transition state $\mathbf{TS4_{5Br}}$, which is 0.4 kcal mol^{-1} less stable than $\mathbf{TS4_{6Br}}$. Finally, the elimination step leads to the complexed 3-pyrroline **7b-Pd** in an exergonic step (by −11.7 kcal mol^{-1}) by overcoming a low activation barrier.

If we compare the free energy profiles for the formation of **6b** and **7b**, a similar profile for the cross-coupling process is found. However, the rate-determining step for **6b** is the cyclization, although very close to the coupling event, whereas for **7b** the cross-coupling is proposed as the rate-determining step, involving a transition structure only 0.1 kcal mol^{-1} higher than the heterocyclization for **6b**. These results are supported by the competitive formation of **6b** and **7b**.

Following the same analysis for the cross-coupling reaction with α-allenic esters **8** to afford dihydropyrans **10** (R = Ph), the calculations reveal critical differences between the formation of the dihydropyran and 3-pyrroline frameworks.

Recently, results of the palladium-catalyzed cross-coupling process between two different allenes (allenol and α-allenic ester) to form dihydropyrans were reported.[18] Computational analysis of the reaction mechanism suggested kinetic control of the chemo- and regioselective intramolecular cyclization. Moreover, the calculations accounted for the absence of the plausible homocoupling, other cross-coupling modes, or Pd–C protonolysis products.

The alkenyl palladium(II) intermediate $\mathbf{I2_6}$ can coordinate an α-allenic ester ligand to form the allene-Pd complex $\mathbf{I3_{6Al}}$ (Figure 3) through an associative mechanism step involving a very low energy barrier (0.9 kcal mol^{-1}) via $\mathbf{TS3_{6Al}}$. This species evolves into complex $\mathbf{I4_{6Al}}$ via the transition state $\mathbf{TS4_{6Al}}$, which shows the incipient formation of a C–C bond with the central carbon of the allene (C–C distance = 2.107 Å). This step proceeds with a low energy barrier ($\Delta G^{\#}$ = 2.7 kcal mol^{-1}) and is strongly exergonic (ΔG = −37.7 kcal mol^{-1}), thus suggesting an irreversible process. It should be noted that $\mathbf{TS4_{6Al}}$ shows a C(sp^2)-H$\cdots\pi$ interaction[19] with the aromatic core (2.504 Å). Other conformations for $\mathbf{TS4_{6Al}}$ and $\mathbf{I4_{6Al}}$ lacking this interaction are 2.8 and 2.7 kcal mol^{-1} higher in energy, respectively (see additional computational results in the Supporting Information).

Finally, a *trans*-β-deacetoxypalladation step drives the formation of *trans*-buta-1,3-dienyl-dihydropyran **10a-Pd** η^4-coordinated to Pd^{II}. This step takes place through transition

DOI: 10.1021/acs.joc.6b00934
J. Org. Chem. 2016, 81, 7362–7372

structure $\mathbf{TS5_{6Al}}$, which shows a C−O cleavage (2.146 Å) and the initial coordination of the ester to the metal (2.951 Å) with an energy 19.8 kcal mol^{-1} below that of $\mathbf{1b\text{-}Pd_D}$. The overall process is highly exergonic (−30.1 kcal mol^{-1}).

A close inspection of the cross-coupling process from the azacycle intermediate $\mathbf{I2_5}$ reveals crucial differences. The corresponding computed reaction profiles are depicted in Figure 3, which collects the relative free energy values calculated at 298 K (ΔG_{298}). Thus, our calculations put forward that the formation of $\mathbf{I3_{5Al}}$ is kinetic (by 1.9 kcal mol^{-1}) and thermodynamically disfavored (by 5.3 kcal mol^{-1}) over the formation of oxacycle $\mathbf{I3_{6Al}}$. Then, the coupling step occurs via transition state $\mathbf{TS4_{5Al}}$, involving the C−C bond formation (2.043 Å) with a free energy 5.5 kcal mol^{-1} higher in energy than that of $\mathbf{TS4_{6Al}}$ in a strong exergonic transformation (ΔG_{298} = −39.0 kcal mol^{-1}). It should be noted that $\mathbf{TS4_{5Al}}$ shows a C(sp^3)-H···π (2.798, 3.211 Å) weaker than a C(sp^2)-H···π in $\mathbf{TS4_{6Al}}$, which could in part account for the higher energy. Finally, we locate the transition state $\mathbf{TS5_{5Al}}$, a saddle point associated with the *trans-β*-deacetoxypalladation step, which leads to the complexed dihydropyrrole product **21-Pd**. Therefore, on the basis of the computed data, it can be concluded that the formation of **10a** seems to be the most favored process for the palladium-catalyzed heterocyclization/cross-coupling sequence between α-allenols and α-allenic esters, taking place with regio- and chemoselectivity, which agrees nicely with the experimental findings.

To account for the differences found between the coupling reagents, we have performed NBO analysis of the coupling processes of allyl bromide and α-allenic acetates. In the intermediate complexes **I3**, the σ-donating (from the endocyclic C_C sp^2 lone pair partially overlapping the 5s orbital on palladium) and π-back-donating (a highly polarized dπ-to-pπ donation from the metal to the empty pπ orbital on C_C) interactions between the heterocyclic scaffold and the catalyst generate a short Pd−endocyclic carbon bond and a high Wiberg bond order (these values exceed the maximum value of 0.5 for a σ bond, see additional computational results in the Supporting Information). This effect is also reflected in the analysis of partial NPA charges, which shows a less NPA negative charge at the PdCl fragment with increasing C_C-Pd bond order. Hence, the charge flow from the π−backbonding interaction of the metal to the alkene/allene moiety should be lower and the interaction weaker. For the coupling process with α-allenic acetate, a comparison of the NBO analysis for $\mathbf{I3_{6Al}}$ and $\mathbf{I3_{5Al}}$ reveals a higher NPA charge at the catalyst (−0.10 vs +0.01e), a lower NPA positive charge at the allene fragment (+0.13 vs +0.03e, respectively), and lower Wiberg bond orders for the Pd-C−allene interactions for $\mathbf{I3_{5Al}}$ (0.222 and 0.198 vs 0.186 and 0.155, respectively), which is also confirmed by the lower interaction energy for $\mathbf{I3_{5Al}}$ than for $\mathbf{I3_{6Al}}$ (ΔE_2 = 7.7 kcal mol^{-1}). Additionally, in the coupling transition state $\mathbf{TS4_{5Al}}$, the analysis also reveals a weaker interaction energy than for $\mathbf{TS4_{6Al}}$ (ΔE_2 = 6.2 kcal mol^{-1}) between the donor π orbital and the empty developing orbital on the endocyclic C_C atom.

In contrast, a comparison of the NBO analysis for $\mathbf{I3_{6Br}}$ and $\mathbf{I3_{5Br}}$ shows a similar negative NPA charge at the catalyst (−0.11 vs −0.12e), an analogous NPA positive charge at the incoming alkene fragment (+0.17 vs +0.19e, respectively), and equivalent Wiberg bond orders for the Pd−alkene interaction (0.246 and 0.218 vs 0.264 and 0.244, respectively). This similarity is reflected by the small difference of interaction energy (slightly lower for $\mathbf{I3_{5Br}}$, ΔE_2 = 1.3 kcal mol^{-1}). Expectedly, the coupling transition structures also reveal similar values for the interaction energy between the donor orbital and the empty developing orbital on the endocyclic C atom. In summary, the results suggest that the interplay of electronic effects at the heterocycle and coupling reagent controls the competitive formation of dihydropyrans and dihydropyrroles in the Pd-catalyzed heterocyclization/cross-coupling reactions of allenic amino alcohols.

CONCLUSIONS

In conclusion, the controlled preparation of 2,5-dihydro-1*H*-pyrroles, 3,6-dihydro-2*H*-pyrans, and pyrroles has been achieved through swithchable chemo- and regioselectivity in the metal-catalyzed heterocyclization reactions of allenic amino alcohols. Chemo- and regioselectivity depend on both the linker elongation as well as the type of catalyst. Furthermore, to justify this different demeanor, density functional theory calculations have been implemented.

EXPERIMENTAL SECTION

General Methods. ^{1}H NMR and ^{13}C NMR spectra were recorded on 300 MHz spectrometers. NMR spectra were recorded in $CDCl_3$ solutions except when stated otherwise. Chemical shifts are given in ppm relative to TMS (^{1}H, 0.0 ppm) or $CDCl_3$ (^{13}C, 77.0 ppm). Low- and high-resolution mass spectra were performed on a QTOF LC−MS spectrometer using the electrospray mode (ES) unless otherwise stated. Specific rotation $[\alpha]_D$ is given in 10^{-1} deg cm^2 g^{-1} at 20 °C, and the concentration (c) is expressed in grams per 100 mL. All commercially available compounds were used without further purification. Flash chromatography was performed by using silica gel 60 (230−400 mesh) or neutral alumina. Products were identified by TLC (silica gel). UV light (λ = 254 nm) and a solution of phosphomolybdic acid in EtOH (1 g of phosphomolybdic acid hydrate, 100 mL EtOH) was used to develop the plates.

Computational Details. The calculations were performed with the Gaussian 09 suite of programs.[20] The structures were optimized with Truhlar's dispersion-corrected meta hybrid exchange-correlation functional M06. This hybrid functional has been recommend for structures involving transition metals.[21,22] The quadruple-ζ quality plus polarization def2-QZVP basis set of Ahlrichs and co-workers[23] has been applied for all atoms except Au and Pd, which were treated with SDD ECPs.[24] The stationary points were characterized by means of harmonic analysis. For all of the transition structures, the normal mode related to the imaginary frequency corresponds to the nuclear motion along the reaction coordinates under study. Additionally, in some cases, we carried out intrinsic reaction coordinate calculations (IRC) to verify that the transition structures connect with reactants and products. The polarizable continuum model (PCM)[25] was applied to consider the solvents effects. Finally, to estimate the changes in the Gibbs energies in the presence of CH_2Cl_2 or DMF as solvent, single-point calculations on the optimized geometries were carried out. The natural bond orbital analysis (NBO)[26] was performed on the optimized structures.

General Procedure for the Deprotection of Allenyloxazolidines 3, 4a, and 4b. *Preparation of N-Boc Allenic Amino Alcohols 1a, 2a, and 2b.* The corresponding allenyloxazolidine **3**, **4a**, or **4b** (1.00 mmol) was dissolved in acetonitrile/water (10 mL, 95:5), and the solution was cooled to 0 °C. $BiCl_3$ (0.05 mmol) was added, and the mixture was stirred at RT until disappearance of the starting material (TLC, typically 14−24 h). The reaction mixture was poured into a sat. aq solution of $NaHCO_3$. The aqueous layer was extracted with ethyl acetate (3 × 20 mL), and the combined organic extracts were dried ($MgSO_4$) and concentrated in vacuo to afford allenic amino alcohols **1a**, **2a**, and **2b**. Further purification was not necessary. Spectroscopic and analytical data for compounds **1a**, **2a**, and **2b** follow.

N-Boc Allenic Amino Alcohol (−)-1a. From 100 mg (0.42 mmol) of allenyloxazolidine (−)-**3**, compound (−)-**1a** (87 mg, quantitative

DOI: 10.1021/acs.joc.6b00934
J. Org. Chem. 2016, 81, 7362−7372

yield) was obtained as a colorless oil; $[\alpha]_D$ −16.2 (*c* 1.2, $CHCl_3$); ^1H NMR (300 MHz, $CDCl_3$, 25 °C) δ 1.43 (s, 9H), 2.86 (br s, 1H), 3.62 (dd, 1H, *J* = 11.1, 5.5 Hz), 3.70 (dd, 1H, *J* = 11.1, 4.1 Hz), 4.23 (br s, 1H), 4.90 (dd, 2H, *J* = 6.7, 3.4 Hz), 4.99 (d, *J* = 7.5 Hz), 5.23 (dd, 1H, *J* = 12.0, 6.5 Hz); ^{13}C NMR (75 MHz, $CDCl_3$, 25 °C) δ 207.2, 156.0, 89.8, 79.8, 78.5, 65.4, 50.7, 28.3; IR ($CHCl_3$, cm^{-1}) ν 3401, 3343, 1959, 1692, 1170; HRMS (ES) calcd for $C_{10}H_{17}NO_3$ $[M]^+$ 199.1208, found 199.1212.

*N-Boc Allenic Amino Alcohol (−)-**2a***. From 100 mg (0.34 mmol) of allenyloxazolidine (−)-**4a**, compound (−)-**2a** (86 mg, quantitative yield) was obtained as a colorless oil; $[\alpha]_D$ −85.5 (*c* 0.5, CH_2Cl_2); ^1H NMR (300 MHz, C_6D_6, 25 °C) δ 1.43 (s, 9H), 1.66 (t, *J* = 3.1 Hz, 3H), 2.98 (s, 3H), 3.60 (dd, *J* = 11.4, 4.0 Hz, 1H), 3.73 (d, *J* = 6.5 Hz, 1H), 3.88 (m, 2H), 4.56 (d, *J* = 1.8 Hz, 2H), 5.02 (d, *J* = 8.5 Hz, 1H); ^{13}C NMR (75 MHz, C_6D_6, 25 °C) δ 207.8, 155.9, 96.5, 83.9, 79.1, 74.8, 62.5, 56.8, 53.3, 28.5 (3C), 13.5; IR ($CHCl_3$, cm^{-1}) ν 3447, 1958, 1695, 1172; HRMS (ES) calcd for $C_{13}H_{23}NO_4$ $[M]^+$ 257.1627, found 257.1628.

*N-Boc Allenic Amino Alcohol (−)-**2b***. From 100 mg (0.28 mmol) of allenyloxazolidine (−)-**4b**, compound (−)-**2b** (89 mg, quantitative yield) was obtained as a colorless oil; $[\alpha]_D$ −23.5 (*c* 0.8, CH_2Cl_2); ^1H NMR (300 MHz, C_6D_6, 25 °C) δ 1.44 (s, 9H), 2.98 (s, 3H), 3.49 (dd, *J* = 11.3, 2.7 Hz, 1H), 3.99 (m, 2H), 4.67 (br s, 1H), 4.88 (m, 2H), 5.53 (d, *J* = 7.6 Hz, 1H), 7.02 (t, *J* = 7.3 Hz, 1H), 7.21 (t, *J* = 7.7 Hz, 2H), 7.72 (d, *J* = 7.6 Hz, 2H); ^{13}C NMR (75 MHz, C C_6D_6, 25 °C) δ 208.8, 156.0, 134.4, 129.0 (2C), 127.5, 127.1 (2C), 104.6, 82.4, 80.0, 79.1, 61.8, 57.6, 54.0, 28.5 (3C); IR ($CHCl_3$, cm^{-1}) ν 3437, 1940, 1703, 1174; HRMS (ES) calcd for $C_{18}H_{25}NO_4$ $[M]^+$ 319.1784, found 319.1773.

Procedure for the La^{III}-Catalyzed Cleavage of *N*-Boc Allene 1a. *Preparation of Allenic Amino Alcohol **1b***. $La[N(SiMe_3)_2]_3$ (0.05 mmol) was added to a stirred solution of the *N*-Boc allenic amino alcohol **1a** (200 mg, 1.0 mmol) in toluene (10.0 mL) under argon. The resulting mixture was stirred at reflux temperature until disappearance of the starting material (TLC, 2 h). The reaction was then filtered through a Celite plug before being concentrated under reduced pressure. Chromatography of the residue eluting with ethyl acetate/hexanes (1:2) gave analytically pure adduct **1b**.

*Allenic Amino Alcohol (+)-**1b***. From 200 mg (1.0 mmol) of *N*-Boc allenic amino alcohol (−)-**1a**, compound (+)-**1b** (99 mg, quantitative yield) was obtained as a colorless oil; $[\alpha]_D$ +9.4 (*c* 0.5, $CHCl_3$); ^1H NMR (300 MHz, $CDCl_3$, 25 °C) δ 4.19 (dd, 1H, *J* = 8.5, 5.6 Hz), 4.42 (dd, 1H, *J* = 13.7, 6.9 Hz), 4.57 (t, 1H, *J* = 8.3 Hz), 4.97 (dt, 2H, *J* = 6.4, 1.7 Hz), 5.22 (dd, 1H, *J* = 13.3, 6.7 Hz), 5.32 (br s, 1H); ^{13}C NMR (75 MHz, $CDCl_3$, 25 °C) δ 208.1, 90.6, 78.8, 70.1, 51.6; IR ($CHCl_3$, cm^{-1}) ν 3279, 1956, 1228; HRMS (ES) calcd for C_5H_9NO $[M]^+$ 99.0684, found 99.0688.

General Procedure for the Indium-Promoted Reaction between 3-Substituted Prop-2-ynyl Bromides and Garner's Aldehyde. Preparation of α-Allenic Alcohols 4a−OH and 4b−OH. 1-Bromo-2-butyne or 1-bromo-3-phenyl-2-propyne (3.0 mmol) was added to a well-stirred suspension of Garner's aldehyde (1.0 mmol) and indium powder (6.0 mmol) in THF/NH_4Cl (aq sat.) (1:5, 5 mL) at 0 °C. After disappearance of the starting material (TLC), the mixture was extracted with ethyl acetate (3 × 5 mL). The organic extract was washed with brine, dried ($MgSO_4$), and concentrated under reduced pressure. Flash chromatography of the residue on deactivated silica gel using an ethyl acetate/hexanes mixtures gave analytically pure compounds.

*α-Allenol (−)-**4a−OH***. From 680 mg (2.96 mmol) of Garner's aldehyde, and after chromatography of the residue using hexanes/ethyl acetate (4:1), compound (−)-**4a−OH** (374 mg, 44%) was obtained as a colorless oil; $[\alpha]_D$ −41.3 (*c* 1.2, CH_2Cl_2); ^1H NMR (300 MHz, C_6D_6, 25 °C) δ 4.63 (m, 2H), 3.70 (m, 4H), 3.36 (t, *J* = 9.8 Hz, 1H), 1.85 (t, *J* = 3.1 Hz, 3H), 1.36 (m, 15H); ^{13}C NMR (75 MHz, C_6D_6, 25 °C) δ 207.9, 155.2, 98.8, 97.4, 79.0, 75.0, 74.8, 63.2, 46.8, 28.8, 28.5 (3C), 19.9, 13.7; IR ($CHCl_3$, cm^{-1}) ν 3478, 1957, 1738; HRMS (ES) calcd for $C_{15}H_{25}NO_4$ $[M]^+$ 283.1784, found 283.1771.

*α-Allenol (−)-**4b−OH***. From 500 mg (2.18 mmol) of Garner's aldehyde, and after chromatography of the residue using hexanes/ethyl acetate (5:1) as eluent, compound (−)-**4b−OH** (411 mg, 54%) was obtained as a colorless oil; $[\alpha]_D$ −39.1 (*c* 1.0, CH_2Cl_2); ^1H NMR (300 MHz, C_6D_6, 25 °C) δ 7.35 (m, 2H), 7.17 (m, 3H), 5.16 (m, 2H), 3.99 (m, 4H), 1.43 (m, 15H); ^{13}C NMR (75 MHz, C_6D_6, 25 °C) δ 208.1, 154.9, 132.0, 128.7 (2C), 128.2, 127.2 (2C), 109.1, 99.4 (2C), 80.0, 72.0, 63.3, 48.0, 28.5, 28.4 (3C), 20.2; IR ($CHCl_3$, cm^{-1}) ν 3476, 1971, 1735; HRMS (ES) calcd for $C_{20}H_{27}NO_4$ $[M]^+$ 345.1940, found 345.1929.

General Procedure for the Synthesis of Methoxy Allenes 4. Tetrabutyl ammonium iodide (cat), 50% aqueous sodium hydroxide (18 mL), and dimethyl sulfate (0.60 mmol) were sequentially added at room temperature to a solution of the corresponding α-allenol (0.92 mmol) in dichloromethane (18 mL). The reaction was stirred until disappearance of the starting material (TLC). Then, aqueous ammonia (30%) was added (2.5 mL) before being partitioned between dichloromethane and water. The aqueous phase was extracted with dichloromethane (3 × 15 mL); the combined organic extracts were dried ($MgSO_4$) and concentrated under reduced pressure. Flash chromatography of the residue on deactivated silica gel using ethyl acetate/hexanes mixtures gave analytically pure compounds.

*Methoxy Allene (−)-**4a***. From 175 mg (0.62 mmol) of α-allenol (−)-**4a−OH**, and after chromatography of the residue using hexanes/ethyl acetate (6:1) as eluent, compound (−)-**4a** (124 mg, 67%) was obtained as a colorless oil; $[\alpha]_D$ −38.9 (*c* 0.9, CH_2Cl_2); ^1H NMR (300 MHz, C_6D_6, 25 °C) δ 4.54 (m, 2H), 3.79 (m, 4H), 3.21 (s, 3H), 1.49 (m, 18H); ^{13}C NMR (75 MHz, C_6D_6, 25 °C) δ 207.9, 155.1, 98.8, 97.4, 79.0, 74.9, 75.0, 63.2, 56.8, 46.8, 28.8, 28.4 (3C), 19.8, 13.7; IR ($CHCl_3$, cm^{-1}) ν 1956, 1737; HRMS (ES) calcd for $C_{16}H_{27}NO_4$ $[M]^+$ 297.1940, found 297.1921.

*Methoxy Allene (−)-**4b***. From 170 mg (0.49 mmol) of α-allenol (−)-**4b−OH**, and after chromatography of the residue using hexanes/ethyl acetate (5:1) as eluent, compound (−)-**4b** (107 mg, 61%) was obtained as a colorless oil; $[\alpha]_D$ −37.1 (*c* 1.5, CH_2Cl_2); ^1H NMR (300 MHz, C_6D_6, 25 °C) δ 7.43 (m, 2H), 7.22 (m, 3H), 5.14 (m, 2H), 4.04 (m, 4H), 3.30 (d, *J* = 9.3 Hz, 3H), 1.37 (m, 15H); ^{13}C NMR (75 MHz, C_6D_6, 25 °C) δ 208.0, 154.9, 131.9, 128.6 (2C), 128.2, 127.2 (2C), 109.0, 99.3 (2C), 79.9, 71.9, 63.2, 57.3, 48.0, 28.4, 28.3 (3C), 20.2; IR ($CHCl_3$, cm^{-1}) ν 1955, 1739; HRMS (ES) calcd for $C_{21}H_{29}NO_4$ $[M]^+$ 359.2097, found 359.2077.

General Procedure for the Au^{III}-Catalyzed Cyclization of α-Amino-β-hydroxyallenes 1. *Preparation of 2,5-Dihydro-1H-pyrroles **5***. $AuCl_3$ (0.025 mmol) was added to a stirred solution of the appropriate allenic amino alcohol **1** (0.50 mmol) in dichloromethane (5 mL) under argon. The resulting mixture was stirred at RT until disappearance of the starting material (TLC, typically 3 h). The reaction was then quenched with brine (0.5 mL); the mixture was extracted with ethyl acetate (3 × 5 mL), and the combined extracts were washed twice with brine. The reaction was concentrated under reduced pressure. Chromatography of the residue eluting with hexanes/ethyl acetate mixtures gave adducts **5**. Spectroscopic and analytical data for pure forms of **5** follow.

*2,5-Dihydro-1H-pyrrole (−)-**5a***. From 44 mg (0.221 mmol) of *N*-Boc allenic amino alcohol (−)-**1a**, and after chromatography of the residue using hexanes/ethyl acetate (4:1) as eluent, compound (−)-**5a** (34 mg, 77%) was obtained as a colorless oil; $[\alpha]_D$ −58.1 (*c* 0.7, $CHCl_3$); ^1H NMR (300 MHz, $CDCl_3$, 25 °C) δ 1.50 (s, 9H), 3.11 (br s, 1H), 3.58 (dd, 1H, *J* = 11.2, 7.0 Hz), 3.79 (dd, 1H, *J* = 11.4, 2.3 Hz), 4.09 (ddt, 1H, *J* = 15.6, 5.4, 2.2 Hz), 4.21 (d, 1H, *J* = 15.4 Hz), 4.71 (br s, 1H), 5.63 (d, 1H, *J* = 4.4 Hz), 5.83 (s, 1H); ^{13}C NMR (75 MHz, $CDCl_3$, 25 °C) δ 156.6, 126.7, 126.6, 80.6, 67.6, 67.3, 54.2, 28.4 (3C); IR ($CHCl_3$, cm^{-1}) ν 3247, 1748, 1207; HRMS (ES) calcd $C_{10}H_{17}NO_3$ $[M]^+$ 199.1208, found 199.1205.

*2,5-Dihydro-1H-pyrrole (+)-**5b***. From 31 mg (0.31 mmol) of α-amino-β-hydroxyallene (+)-**1b**, and after chromatography of the residue using hexanes/ethyl acetate (2:1) as eluent, compound (+)-**5b** (25 mg, 81%) was obtained as a colorless oil; $[\alpha]_D$ +5.4 (*c* 0.5, $CHCl_3$); ^1H NMR (300 MHz, $CDCl_3$, 25 °C) δ 3.83 (m, 1H), 4.25 (dd, 1H, *J* = 8.5, 5.1 Hz), 4.40 (ddt, 1H, *J* = 15.6, 3.0, 2.1 Hz), 4.61 (t, 1H, *J* = 8.6 Hz), 4.74 (m, 1H), 5.91 (dt, 1H, *J* = 5.9, 2.9 Hz), 6.06 (ddd, 1H, *J* = 5.9, 3.7, 2.1 Hz); ^{13}C NMR (75 MHz, $CDCl_3$, 25

DOI: 10.1021/acs.joc.6b00934
J. Org. Chem. 2016, 81, 7362−7372

°C) δ 130.9, 128.9, 68.7, 64.6, 54.8; IR ($CHCl_3$, cm^{-1}) ν 3325, 1247; HRMS (ES) calcd C_5H_9NO $[M]^+$ 99.0684, found 99.0687.

General Procedure for the Pd^{II}-Catalyzed Cyclization of α-Amino-β-hydroxyallenes 1 in the Presence of Allyl Bromide. *Preparation of Dihydropyrans* ***6*** *and Dihydropyrroles* ***7***. Palladium(II) chloride (0.005 mmol) was added to a stirred solution of corresponding allenic amino alcohol **1** (0.10 mmol) and allyl bromide (0.25 mmol) in *N*,*N*-dimethylformamide (1.0 mL). The reaction was stirred under an argon atmosphere until disappearance of the starting material (TLC, 2 h). Water (0.5 mL) was added before being extracted with ethyl acetate (3 × 4 mL). The organic phase was washed with water (2 × 2 mL), dried ($MgSO_4$), and concentrated under reduced pressure. Chromatography of the residue eluting with hexanes/ethyl acetate mixtures gave analytically pure adducts **6** and **7**.

*Preparation of Dihydropyran (−)-**6a** and Dihydropyrrole (+)-**7a***. From 40 mg (0.20 mmol) of α-amino-β-hydroxyallene (−)-**1a**, and after chromatography of the residue using hexanes/ethyl acetate (4:1) as eluent, 22 mg (45%) of the less polar compound (−)-**6a** and 10 mg (21%) of the more polar compound (+)-**7a** were obtained.

*Dihydropyran (−)-**6a***. Colorless oil; $[\alpha]_D$ −47.8 (*c* 0.7, $CHCl_3$); ^1H NMR (300 MHz, $CDCl_3$, 25 °C) δ 1.45 (s, 9H), 2.67 (d, 2H, *J* = 6.8 Hz), 3.66 (dd, 1H, *J* = 11.4, 3.0 Hz), 3.79 (d, 1H, *J* = 12.0 Hz), 4.01 (m, 2H), 4.78 (d, 1H, *J* = 8.2 Hz), 5.08 (m, 2H), 5.59 (s, 1H), 5.75 (ddt, 1H, *J* = 16.4, 9.4, 6.9 Hz); ^{13}C NMR (75 MHz, $CDCl_3$, 25 °C) δ 155.1, 139.6, 134.5, 119.6, 117.2, 79.4, 69.4, 67.6, 44.2, 37.3, 28.4 (3C); IR ($CHCl_3$, cm^{-1}) ν 3301, 1737, 1215; HRMS (ES) calcd $C_{13}H_{21}NO_3$ $[M]^+$ 239.1521, found 239.1531.

*Dihydropyrrole (+)-**7a***. Colorless oil; $[\alpha]_D$ +26.7 (*c* 0.4, $CHCl_3$); ^1H NMR (300 MHz, $CDCl_3$, 25 °C) δ 1.49 (s, 9H), 2.84 (d, 2H, *J* = 6.6 Hz), 3.56 (dd, 1H, *J* = 11.4, 7.2 Hz), 3.75 (dd, 1H, *J* = 11.4, 2.2 Hz), 4.04 (m, 2H), 4.70 (br s, 1H), 5.09 (s, 1H), 5.14 (m, 1H), 5.30 (m, 1H), 5.81 (m, 1H); ^{13}C NMR (75 MHz, $CDCl_3$, 25 °C) δ 156.6, 139.2, 134.1, 120.4, 117.2, 80.6, 68.1, 67.6, 55.8, 33.2, 28.5; IR ($CHCl_3$, cm^{-1}) ν 2992, 1754, 1188; HRMS (ES) calcd $C_{13}H_{21}NO_3$ $[M]^+$ 239.1521, found 239.1523.

*Preparation of Dihydropyran (−)-**6b** and Dihydropyrrole (+)-**7b***. From 50 mg (0.50 mmol) of α-amino-β-hydroxyallene (+)-**1b**, and after chromatography of the residue using hexanes/ethyl acetate (4:1) as eluent, 37 mg (53%) of the less polar compound (−)-**6b** and 28 mg (39%) of the more polar compound (+)-**7b** were obtained.

*Dihydropyran (−)-**6b***. Colorless oil; $[\alpha]_D$ −16.2 (*c* 0.4, $CHCl_3$); ^1H NMR (300 MHz, $CDCl_3$, 25 °C) δ 2.90 (d, 2H, *J* = 6.6 Hz), 3.77 (m, 1H), 4.22 (dd, 1H, *J* = 8.5, 5.2 Hz), 4.25 (m, 1H), 4.57 (t, 1H, *J* = 8.6 Hz), 4.74 (m, 1H), 5.13 (m, 2H), 5.53 (m, 1H), 5.81 (m, 1H); ^{13}C NMR (75 MHz, $CDCl_3$, 25 °C) δ 144.3, 133.6, 122.7, 117.5, 69.0, 64.8, 56.5, 33.1; IR ($CHCl_3$, cm^{-1}) ν 3278, 1231; HRMS (ES) calcd $C_8H_{13}NO$ $[M]^+$ 139.0997, found 139.0998.

*Dihydropyrrole (+)-**7b***. Colorless oil; $[\alpha]_D$ +10.4 (*c* 0.3, $CHCl_3$); ^1H NMR (300 MHz, $CDCl_3$, 25 °C) δ 2.99 (d, 2H, *J* = 6.2 Hz), 4.03 (m, 1H), 4.05 (dd, 1H, *J* = 8.5, 7.0 Hz), 4.54 (t, 1H, *J* = 8.5 Hz), 4.70 (m, 1H), 5.10 (m, 2H), 5.19 (m, 1H), 5.70 (m, 1H), 5.76 (m, 1H); ^{13}C NMR (75 MHz, $CDCl_3$, 25 °C) δ 139.3, 134.3, 128.8, 117.1, 69.8, 50.0, 48.2, 32.7; IR ($CHCl_3$, cm^{-1}) ν 2920, 1188; HRMS (ES) calcd $C_8H_{13}NO$ $[M]^+$ 139.0997, found 139.1006.

General Procedure for the Pd^{II}-Catalyzed Cyclization of α-Amino-β-hydroxyallenes 1 in the Presence of α-Allenic Acetates 8. *Preparation of Dihydropyrans* ***9*** *and* ***10***. Palladium(II) chloride (0.005 mmol) was added to a stirred solution of the appropriate allenic amino alcohol **1** (0.10 mmol) and the correspondinge α-allenic acetate **8** (0.30 mmol) in *N*,*N*-dimethylformamide (1.0 mL). The reaction was stirred under argon atmosphere until disappearance of the starting material (TLC). Water (0.5 mL) was added before being extracted with ethyl acetate (3 × 4 mL). The organic phase was washed with water (2 × 2 mL), dried ($MgSO_4$), and concentrated under reduced pressure. Chromatography of the residue eluting with hexanes/ethyl acetate mixtures gave analytically pure 3,6-dihydro-2*H*-pyran-3-amine derivatives **9** and **10**.

*Dihydropyran (−)-**9a***. From 50 mg (0.25 mmol) of *N*-Boc allenic amino alcohol (−)-**1a**, and after chromatography of the residue using hexanes/ethyl acetate (5:1) as eluent, compound (−)-**9a** (38 mg, 44%) was obtained as a colorless oil; $[\alpha]_D$ −1.2 (*c* 1.3, $CHCl_3$); ^1H NMR (300 MHz, $CDCl_3$, 25 °C) δ 1.46 (s, 9H), 2.01 (d, 3H, *J* = 1.3 Hz), 3.79 (m, 2H), 4.22 (m, 2H), 4.85 (d, 1H, *J* = 8.1 Hz), 5.01 (d, 1H, *J* = 1.0 Hz), 5.17 (d, 1H, *J* = 1.12 Hz), 5.84 (d, 1H, *J* = 4.3 Hz), 6.52 (s, 1H), 7.30 (m, 5H); ^{13}C NMR (75 MHz, $CDCl_3$, 25 °C) δ 155.2, 150.0, 140.2, 137.6, 136.5, 129.7, 129.1 (2C), 128.1 (2C), 126.7, 123.2, 112.5, 79.6, 69.4, 67.3, 44.2, 28.4 (3C), 17.0; IR ($CHCl_3$, cm^{-1}) ν 3343, 1709, 1236; HRMS (ES) calcd $C_{17}H_{19}NO_3$ [M − isobutene + H]$^+$ 286.1443, found 286.1451.

*Dihydropyran (−)-**9b***. From 50 mg (0.25 mmol) of *N*-Boc allenic amino alcohol (−)-**1a**, and after chromatography of the residue using hexanes/ethyl acetate (4:1) as eluent, compound (−)-**9b** (44 mg, 47%) was obtained as a colorless oil; $[\alpha]_D$ −17.1 (*c* 0.6, $CHCl_3$); ^1H NMR (300 MHz, $CDCl_3$, 25 °C) δ 1.45 (s, 9H), 2.00 (d, 3H, *J* = 1.2 Hz), 3.81 (m, 2H), 3.83 (s, 3H), 4.24 (m, 2H), 4.85 (d, 1H, *J* = 8.3 Hz), 4.99 (s, 1H), 5.14 (s, 1H), 5.82 (d, 1H, *J* = 4.1 Hz), 6.45 (s, 1H), 6.90 (d, 2H, *J* = 8.8 Hz), 7.25 (d, 2H, *J* = 8.7 Hz); ^{13}C NMR (75 MHz, $CDCl_3$, 25 °C) δ 159.3, 158.3, 150.2, 134.9, 131.7, 130.3 (2C), 129.2, 127.1, 123.1, 113.6 (2C), 112.2, 81.4, 69.0, 67.4, 55.3, 44.2, 28.4 (3C), 17.0; IR ($CHCl_3$, cm^{-1}) ν 3237, 1718, 1195; HRMS (ES) calcd $C_{22}H_{29}NO_4$ $[M]^+$ 371.2097, found 371.2099.

*Dihydropyran (−)-**10a***. From 50 mg (0.5 mmol) of α-amino-β-hydroxyallene (+)-**1b**, and after chromatography of the residue using hexanes/ethyl acetate (5:1) as eluent, compound (−)-**10a** (68 mg, 56%) was obtained as a colorless oil; $[\alpha]_D$ −5.7 (*c* 1.4, $CHCl_3$); ^1H NMR (300 MHz, $CDCl_3$, 25 °C) δ 1.98 (d, 3H, *J* = 1.4 Hz_3), 4.02 (ddd, 1H, *J* = 14.7, 4.2, 2.3 Hz), 4.28 (dd, 1H, *J* = 8.6, 5.0 Hz), 4.58 (ddd, 1H, *J* = 14.7, 2.7, 1.6 Hz), 4.62 (t, 1H, *J* = 8.7 Hz), 4.87 (m, 1H), 5.11 (s, 1H), 5.27 (s, 1H), 5.83 (q, 1H, *J* = 1.7 Hz), 6.48 (s, 1H), 7.32 (m, 5H); ^{13}C NMR (75 MHz, $CDCl_3$, 25 °C) δ 146.1, 143.4, 137.4, 136.7, 129.3, 129.0 (2C), 128.2 (2C), 126.8, 125.9, 115.1, 68.6, 65.2, 55.1, 18.1; IR ($CHCl_3$, cm^{-1}) ν 3454, 1236; HRMS (ES) calcd $C_{16}H_{19}NO$ $[M]^+$ 241.1467, found 241.1475.

*Dihydropyran (−)-**10b***. From 50 mg (0.5 mmol) of α-amino-β-hydroxyallene (+)-**1b**, and after chromatography of the residue using hexanes/ethyl acetate (4:1) as eluent, compound (−)-**10b** (71 mg, 52%) was obtained as a colorless oil; $[\alpha]_D$ −1.8 (*c* 1.2, $CHCl_3$); ^1H NMR (300 MHz, $CDCl_3$, 25 °C) δ 1.05 (d, 3H, *J* = 1.3 Hz), 3.83 (s, 3H), 4.01 (ddd, 1H, *J* = 14.7, 4.2, 2.3 Hz), 4.28 (dd, 1H, *J* = 8.6, 5.1 Hz), 4.57 (ddd, 1H, *J* = 14.7, 2.7, 1.6 Hz), 4.61 (t, 1H, *J* = 8.7 Hz), 4.86 (m, 1H), 5.09 (s, 1H), 5.24 (s, 1H), 5.81 (q, 1H, *J* = 1.7 Hz), 6.41 (s, 1H), 6.90 (d, 2H, *J* = 8.8 Hz), 7.26 (d, 2H, *J* = 7.1 Hz); ^{13}C NMR (75 MHz, $CDCl_3$, 25 °C) δ 163.2, 146.3, 143.6, 135.0, 130.2 (2C), 130.0, 128.8, 125.8, 114.8, 113.7 (2C), 68.7, 65.2, 55.3, 55.2, 18.0; IR ($CHCl_3$, cm^{-1}) ν 3461, 1228; HRMS (ES) calcd $C_{17}H_{21}NO_2$ $[M]^+$ 271.1572, found 271.1580.

General Procedure for the Au^{I}-Catalyzed Cyclization of β-Amino-γ-hydroxyallenes 2. *Preparation of Pyrroles* ***11***. [(Ph_3P)-$AuNTf_2$] (0.05 mmol) was added to a stirred solution of the corresponding allenic amino alcohol **2** (1.0 mmol) in dichloromethane (4.0 mL) under argon. The resulting mixture was stirred at room temperature until disappearance of the starting material (TLC, typically 2 h). After filtration through a pad of Celite, the mixture was extracted with dichloromethane (3 × 10 mL), and the combined extracts were washed twice with brine. The organic layer was dried ($MgSO_4$) and concentrated under reduced pressure. Chromatography (deactivated silica gel or neutral alumina) of the residue eluting with ethyl acetate/hexanes mixtures gave adducts **11**.

*Pyrrole **11a***. From 70 mg (0.27 mmol) of β-amino-γ-hydroxyallene **2a**, and after chromatography of the residue using hexanes/ethyl acetate (3:1) as eluent, compound **11a** (32 mg, 53%) was obtained as a colorless oil; ^1H NMR (300 MHz, C_6D_6, 25 °C) δ 5.85 (s, 1H), 4.68 (s, 2H), 3.47 (br s, 1H), 2.11 (s, 3H), 1.82 (s, 3H), 1.22 (s, 9H); ^{13}C NMR (75 MHz, C_6D_6, 25 °C) δ 151.3, 134.9, 127.4, 118.3, 115.4, 83.5, 58.8, 27.7 (3C), 13.6, 11.2 (CH_3); IR ($CHCl_3$, cm^{-1}) ν 3441, 2927, 1733, 1366, 1327, 1139; HRMS (ES) calcd $C_{12}H_{19}NO_3$ $[M]^+$ 225.1365, found 225.1368.

*Pyrrole **11b***. From 85 mg (0.18 mmol) of β-amino-γ-hydroxyallene **2b**, and after chromatography of the residue using hexanes/ethyl acetate (3:1) as eluent, compound **11a** (20 mg, 40%) was obtained as

DOI: 10.1021/acs.joc.6b00934
J. Org. Chem. 2016, 81, 7362−7372

a colorless oil; ^{1}H NMR (300 MHz, C_6D_6, 25 °C) δ 7.35 (m, 2H),7.26 (m, 3H), 6.16 (s, 1H), 4.67 (s, 2H), 2.27 (s, 3H), 1.22 (s, 9H); ^{13}C NMR (75 MHz, C_6D_6, 25 °C) δ 151.3, 136. 5, 135.6, 129.2 (2C), 128.9, 128.8 (2C), 126.7, 125.8, 114.1, 84.0, 58.7, 27.7 (3C), 14.7; IR ($CHCl_3$, cm^{-1}) ν 3394, 2977, 1737, 1366, 1327, 1132; HRMS (ES) calcd $C_{17}H_{21}NO_3$ $[M]^+$ 287.1521, found 287.1535.

■ ASSOCIATED CONTENT

Supporting Information

The Supporting Information is available free of charge on the ACS Publications website at DOI: 10.1021/acs.joc.6b00934.

Copies of NMR spectra of new compounds, additional computational results, and Cartesian coordinates (PDF)

■ AUTHOR INFORMATION

Corresponding Authors

*E-mail: alcaideb@quim.ucm.es.

*E-mail: Palmendros@iqog.csic.es.

Notes

The authors declare no competing financial interest.

■ ACKNOWLEDGMENTS

Financial support for this work from MINECO and FEDER (Projects CTQ2012-33664-C02-01, CTQ2012-33664-C02-02, CTQ2015-65060-C2-1-P, and CTQ2015-65060-C2-2-P) is gratefully acknowledged. E.S. thanks CESGA (USC) and CTI-CSIC for supercomputing time.

■ REFERENCES

(1) For recent reviews on allene chemistry, see: (a) Yang, W.; Hashmi, A. S. K. *Chem. Soc. Rev.* **2014**, *43*, 2941. (b) Lechel, T.; Pfrengle, F.; Reissig, H.-U.; Zimmer, R. *ChemCatChem* **2013**, *5*, 2100. (c) Yu, S.; Ma, S. *Angew. Chem., Int. Ed.* **2012**, *51*, 3074. (d) Hashmi, A. S. K. *Angew. Chem., Int. Ed.* **2000**, *39*, 3590.

(2) For the first gold-catalyzed conversion of allenes, see: Hashmi, A. S. K.; Schwarz, L.; Choi, J. H.; Frost, T. M. *Angew. Chem., Int. Ed.* **2000**, *39*, 2285.

(3) Winter, C.; Krause, N. *Angew. Chem., Int. Ed.* **2009**, *48*, 6339.

(4) For other selectivity switches in transition metal catalysis, see for example: (a) Hashmi, A. S. K.; Schwarz, L.; Bats, J. W. *J. Prakt. Chem.* **2000**, *342*, 40. For competing nucleophiles in similar distance, see: (b) Hashmi, A. S. K.; Haufe, P.; Schmid, C.; Nass, A. R.; Frey, W. *Chem. - Eur. J.* **2006**, *12*, 5376. (c) Hashmi, A. S. K.; Schuster, A. M.; Gaillard, S.; Cavallo, L.; Poater, A.; Nolan, S. P. *Organometallics* **2011**, *30*, 6328.

(5) Hashmi, A. S. K. *Angew. Chem., Int. Ed.* **2010**, *49*, 5232.

(6) Alcaide, B.; Almendros, P.; Quirós, M. T.; Fernández, I. *Beilstein J. Org. Chem.* **2013**, *9*, 818.

(7) Alcaide, B.; Almendros, P.; Cembellín, S.; Martínez del Campo, T.; Fernández, I. *Chem. Commun.* **2013**, *49*, 1282.

(8) For the gold-catalyzed cycloisomerization of α-aminoallenes to pyrrolines, see: (a) Morita, N.; Krause, N. *Eur. J. Org. Chem.* **2006**, *2006*, 4634. (b) Morita, N.; Krause, N. *Org. Lett.* **2004**, *6*, 4121.

(9) For the palladium-catalyzed cyclization of heterosubstituted allenes in the presence of allylic halides, see: (a) Ma, S.; Yu, F.; Gao, W. *J. Org. Chem.* **2003**, *68*, 5943. (b) Ma, S.; Gao, W. *J. Org. Chem.* **2002**, *67*, 6104. (c) Ma, S.; Gao, W. *Tetrahedron Lett.* **2000**, *41*, 8933.

(10) Alcaide, B.; Almendros, P.; Martínez del Campo, T. *Angew. Chem., Int. Ed.* **2006**, *45*, 4501.

(11) (a) Arredondo, V. M.; McDonald, F. E.; Marks, T. J. *J. Am. Chem. Soc.* **1998**, *120*, 4871. (b) Kim, Y. K.; Livinghouse, T.; Bercaw, J. E. *Tetrahedron Lett.* **2001**, *42*, 2933. (c) Burgstein, M. R.; Berberich, H.; Roesky, P. W. *Chem. - Eur. J.* **2001**, *7*, 3078. (d) Hong, S.; Marks, T. J. *Acc. Chem. Res.* **2004**, *37*, 673. (e) Tobisch, S. *Chem. - Eur. J.* **2006**, *12*, 2520.

(12) (a) Yu, X.; Seo, S.; Marks, T. J. *J. Am. Chem. Soc.* **2007**, *129*, 7244. (b) Seo, S.; Yu, X.; Marks, T. J. *J. Am. Chem. Soc.* **2009**, *131*, 263. (c) Alcaide, B.; Almendros, P.; Martínez del Campo, T.; Soriano, E.; Marco-Contelles, J. L. *Chem. - Eur. J.* **2009**, *15*, 1901. (d) Alcaide, B.; Almendros, P.; Martínez del Campo, T.; Soriano, E.; Marco-Contelles, J. L. *Chem. - Eur. J.* **2009**, *15*, 1909.

(13) (a) Tan, S. M.; Willis, A. C.; Paddon-Row, M. N.; Sherburn, M. S. *Angew. Chem., Int. Ed.* **2016**, *55*, 3081. (b) Kobayashi, S.; Kudo, K.; Ito, A.; Hirama, S.; Otani, T.; Saito, T. *Org. Biomol. Chem.* **2014**, *12*, 4061. (c) Kobayashi, S.; Furuya, T.; Otani, T.; Saito, T. *Tetrahedron Lett.* **2008**, *49*, 4513. (d) Dion, A.; Dubé, P.; Spino, C. *Org. Lett.* **2005**, *7*, 5601.

(14) (a) Marshall, J. A.; Wang, X.-J. *J. Org. Chem.* **1990**, *55*, 2995. (b) Schierle, K.; Vahle, R.; Steckhan, E. *Eur. J. Org. Chem.* **1998**, *1998*, 509. (c) Billet, M.; Schoenfelder, A.; Klotz, P.; Mann, A. *Tetrahedron Lett.* **2002**, *43*, 1453. (d) Hashmi, A. S. K.; Blanco, M. C.; Fischer, D.; Bats, J. W. *Eur. J. Org. Chem.* **2006**, *2006*, 1387. (e) Gockel, B.; Krause, N. *Org. Lett.* **2006**, *8*, 4485. (f) Asikainen, M.; Krause, N. *Adv. Synth. Catal.* **2009**, *351*, 2305. (g) Eom, D.; Kang, D.; Lee, P. H. *J. Org. Chem.* **2010**, *75*, 7447.

(15) Alcaide, B.; Almendros, P.; Martínez del Campo, T.; Quirós, M. T.; Soriano, E.; Marco-Contelles, J. L. *Chem. - Eur. J.* **2009**, *15*, 9127.

(16) Zhu, R.-X.; Zhang, D.-J.; Guo, J.-X.; Mu, J.-L.; Duan, C.-G.; Liu, C.-B. *J. Phys. Chem. A* **2010**, *114*, 4689.

(17) The participation of the chloride ligands has been described previously, see: (a) Lemière, G.; Gandon, V.; Agenet, N.; Goddard, J.-P.; de Kozak, A.; Aubert, C.; Fensterbank, L.; Malacria, M. *Angew. Chem., Int. Ed.* **2006**, *45*, 7596. (b) Xia, Y.; Dudnik, A. S.; Gevorgyan, V.; Li, Y. *J. Am. Chem. Soc.* **2008**, *130*, 6940.

(18) Alcaide, B.; Almendros, P.; Martínez del Campo, T.; Soriano, E.; Marco-Contelles, J. L. *Chem. - Eur. J.* **2013**, *19*, 14233.

(19) Scheiner, S. *Hydrogen Bonding: A Theoretical Perspective*; Oxford University Press, 1997.

(20) Frisch, M. J.; Trucks, G. W.; Schlegel, H. B.; Scuseria, G. E.; Robb, M. A.; Cheeseman, J. R.; Scalmani, G.; Barone, V.; Mennucci, B.; Petersson, G. A.; Nakatsuji, H.; Caricato, M.; Li, X.; Hratchian, H. P.; Izmaylov, A. F.; Bloino, J.; Zheng, G.; Sonnenberg, J. L.; Hada, M.; Ehara, M.; Toyota, K.; Fukuda, R.; Hasegawa, J.; Ishida, M.; Nakajima, T.; Honda, Y.; Kitao, O.; Nakai, H.; Vreven, T.; Montgomery, J. A.; Peralta, J. E., Jr.; Ogliaro, F.; Bearpark, M.; Heyd, J. J.; Brothers, E.; Kudin, K. N.; Staroverov, V. N.; Keith, T.; Kobayashi, R.; Normand, J.; Raghavachari, K.; Rendell, A.; Burant, J. C.; Iyengar, S. S.; Tomasi, J.; Cossi, M.; Rega, N.; Millam, J. M.; Klene, M.; Knox, J. E.; Cross, J. B.; Bakken, V.; Adamo, C.; Jaramillo, J.; Gomperts, R.; Stratmann, R. E.; Yazyev, O.; Austin, A. J.; Cammi, R.; Pomelli, C.; Ochterski, J. W.; Martin, R. L.; Morokuma, K.; Zakrzewski, V. G.; Voth, G. A.; Salvador, P.; Dannenberg, J. J.; Dapprich, S.; Daniels, A. D.; Farkas, O.; Foresman, J. B.; Ortiz, J. V.; Cioslowski, J.; Fox, D. J. *Gaussian 09*, revision D.01; Gaussian, Inc.: Wallingford, CT, 2013.

(21) (a) Zhao, Y.; Truhlar, D. G. *Acc. Chem. Res.* **2008**, *41*, 157. (b) Zhao, Y.; Truhlar, D. G. *Theor. Chem. Acc.* **2008**, *120*, 215.

(22) (a) Faza, O. N.; López, C. S. *Top. Curr. Chem.* **2014**, *357*, 213. (b) Nieto-Faza, O.; Álvarez-Rodríguez, R.; Silva-López, C. *Theor. Chem. Acc.* **2011**, *128*, 647. (c) Kang, R.; Chen, H.; Shaik, S.; Yao, J. *J. Chem. Theory Comput.* **2011**, *7*, 4002.

(23) Weigend, F.; Ahlrichs, R. *Phys. Chem. Chem. Phys.* **2005**, *7*, 3297.

(24) Andrae, D.; Haeussermann, U.; Dolg, M.; Stoll, H.; Preuss, H. *Theor. Chim. Acta* **1990**, *77*, 123.

(25) (a) Miertus, S.; Scrocco, E.; Tomasi, J. *Chem. Phys.* **1981**, *55*, 117. (b) Pascual-Ahuir, J. L.; Silla, E.; Tuñón, I. *J. Comput. Chem.* **1994**, *15*, 1127. (c) Barone, V.; Cossi, M. *J. Phys. Chem. A* **1998**, *102*, 1995.

(26) (a) Reed, A. E.; Weinhold, F. *J. Chem. Phys.* **1985**, *83*, 1736. (b) Reed, A. E.; Weinstock, R. B.; Weinhold, F. *J. Chem. Phys.* **1985**, *83*, 735. (c) Reed, A. E.; Curtiss, L. A.; Weinhold, F. *Chem. Rev.* **1988**, *88*, 899.

DOI: 10.1021/acs.joc.6b00934
J. Org. Chem. 2016, 81, 7362−7372